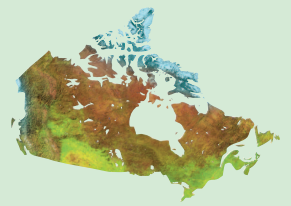




Natural Resources
Canada

Ressources naturelles
Canada



New U-Pb geochronological results from plutonic and sedimentary rocks of Southampton Island, Nunavut

N. Rayner, J. Chakungal, and M. Sanborn-Barrie

Geological Survey of Canada

Current Research 2011-5

2011

**Geological Survey of Canada
Current Research 2011-5**



**New U-Pb geochronological results
from plutonic and sedimentary rocks of
Southampton Island, Nunavut**

N. Rayner, J. Chakungal, and M. Sanborn-Barrie

2011

©Her Majesty the Queen in Right of Canada 2011

ISSN 1701-4387
Catalogue No. M44-2011/5E-PDF
ISBN 978-1-100-17574-4
doi: 10.4095/287286

A copy of this publication is also available for reference in depository libraries across Canada through access to the Depository Services Program's Web site at <http://dsp-psd.pwgsc.gc.ca>

A free digital download of this publication is available from GeoPub:
http://geopub.nrcan.gc.ca/index_e.php

Toll-free (Canada and U.S.A.): 1-888-252-4301

Recommended citation

Rayner, N., Chakungal, J., and Sanborn-Barrie, M., 2011. New U-Pb geochronological results from plutonic and sedimentary rocks of Southampton Island, Nunavut; Geological Survey of Canada, Current Research 2011-5, 20 p. doi:10.4095/287286

Critical review

N. Joyce

Authors

N. Rayner
(Nicole.Rayner@NRCan-RNCan.gc.ca)
M. Sanborn-Barrie
(Mary.Sanborn-Barrie@NRCan-RNCan.gc.ca)
Geological Survey of Canada
601 Booth Street
Ottawa, Ontario
K1A 0E8

J. Chakungal
(joyia.chakungal@gov.yk.ca)
Yukon Geological Survey
2099-2nd Avenue
Whitehorse, Yukon
Y1A 1B5

Correction date:

**All requests for permission to reproduce this work, in whole or in part, for purposes of commercial use, resale, or redistribution shall be addressed to: Earth Sciences Sector Copyright Information Officer, Room 644B, 615 Booth Street, Ottawa, Ontario K1A 0E9.
E-mail: ESSCopyright@NRCan.gc.ca**

New U-Pb geochronological results from plutonic and sedimentary rocks of Southampton Island, Nunavut

N. Rayner, J. Chakungal, and M. Sanborn-Barrie

Rayner, N., Chakungal, J., and Sanborn-Barrie, M., 2011. New U-Pb geochronological results from plutonic and sedimentary rocks of Southampton Island, Nunavut; Geological Survey of Canada, Current Research 2011-5, 20 p. doi:10.4095/287286

Abstract: A hornblende-biotite monzogranite with a crystallization age of 2692 ± 6 Ma and semipelite-psammite cut by a peraluminous granite dated at 2682 ± 17 Ma establish the presence of plutonic and supracrustal rocks of Archean age on Southampton Island. A potentially Paleoproterozoic carbonate-quartzite cover sequence has a maximum depositional age of 2615 ± 23 Ma, similar to an epiclastic rock (2599 ± 15 Ma) that differs in provenance profile. A quartz porphyry is dated at 1934 ± 8 Ma, similar in age to charnockite dated at 1931 ± 19 Ma. A sample of gabbroic anorthosite is interpreted to have crystallized at 1870 ± 10 Ma. Regionally extensive, foliated biotite granodiorite is dated at 1852 ± 8 Ma. Archean detritus and inheritance, as old as 3.7 Ga, is common in the aforementioned metasedimentary and plutonic rocks, with the exception of the quartz porphyry. Massive to very weakly foliated monzogranite, dated at 1821.7 ± 2.5 Ma, provides a minimum age on penetrative deformation across Southampton Island.

Résumé : Un monzogranite à hornblende-biotite ayant un âge de cristallisation de 2692 ± 6 Ma ainsi qu'une semipélite-psammite recoupée par un granite hyperalumineux datant de 2682 ± 17 Ma témoignent de la présence de roches plutoniques et de roches supracrustales de l'Archéen dans l'île Southampton. Une séquence de couverture de roches carbonatées-quartzite, probablement du Paléoprotérozoïque, possède un âge de dépôt maximal de 2615 ± 23 Ma, lequel est semblable à celui d'une roche épicyclastique (2599 ± 15 Ma) affichant un spectre de provenance différent. L'âge d'un porphyre à quartz est évalué à 1934 ± 8 Ma et est semblable à celui d'une charnockite datée à 1931 ± 19 Ma. L'âge de cristallisation d'un échantillon d'anorthosite gabbroïque s'établirait à 1870 ± 10 Ma. Une granodiorite à biotite foliée d'étendue régionale est datée à 1852 ± 8 Ma. Des débris et un héritage de l'Archéen, dont les âges peuvent être aussi anciens que 3,7 Ga, sont révélés fréquemment dans les roches plutoniques et métasédimentaires susmentionnées, sauf dans le porphyre à quartz. Un monzogranite massif à faiblement folié, daté à $1821,7 \pm 2,5$ Ma, permet d'établir un âge minimal pour la déformation pénétrative dans l'île Southampton.

GEOLOGICAL BACKGROUND

Southampton Island, situated at the junction between the Rae craton and Meta Incognita terrane (Fig. 1), exposes a highland of plutonic-dominated Precambrian rock across its eastern half. The exposed basement comprises remnants of a psammite and semipelite sequence with associated iron formation, a carbonate-quartzite sequence, and voluminous plutonic rocks ranging from ultramafic to monzogranitic compositions (Fig. 2; Sanborn-Barrie et al., 2007, 2008, 2009; Chakungal et al., 2007, 2008). Recent mapping indicates that metasedimentary rocks are typically associated with, and locally cut by, mafic plutonic rocks that include layered peridotite-gabbro-gabbroic anorthosite. These have been subsequently intruded by regionally voluminous granodiorite-tonalite-monzogranite±monzonite intrusions.

Amphibolite-facies metamorphism is widespread, with local evidence for an earlier, high-temperature granulite-facies event. The penetrative nature of Paleoproterozoic tectonometamorphism across the island is highlighted by direct U-Pb monazite dating (Berman et al., in press). D_1 is recognized by a penetrative, moderately to steeply inclined, north-trending planar fabric (S_1) defined in places by granulite-facies mineral assemblages that developed at ca. 1.88 Ga. Between 1.86 and 1.84 Ga, S_1 was strongly reworked (D_2) into recumbent, west-trending, south-vergent F_2 folds and/or relatively straight panels of gently inclined, west-striking S_1+S_2 transposition foliation. Broad, open, northeast-trending upright folds (F_3) of the transposition foliation manifest a non-penetrative component of shortening (D_3) (Sanborn-Barrie et al., 2007, 2008; Chakungal et al., 2007).

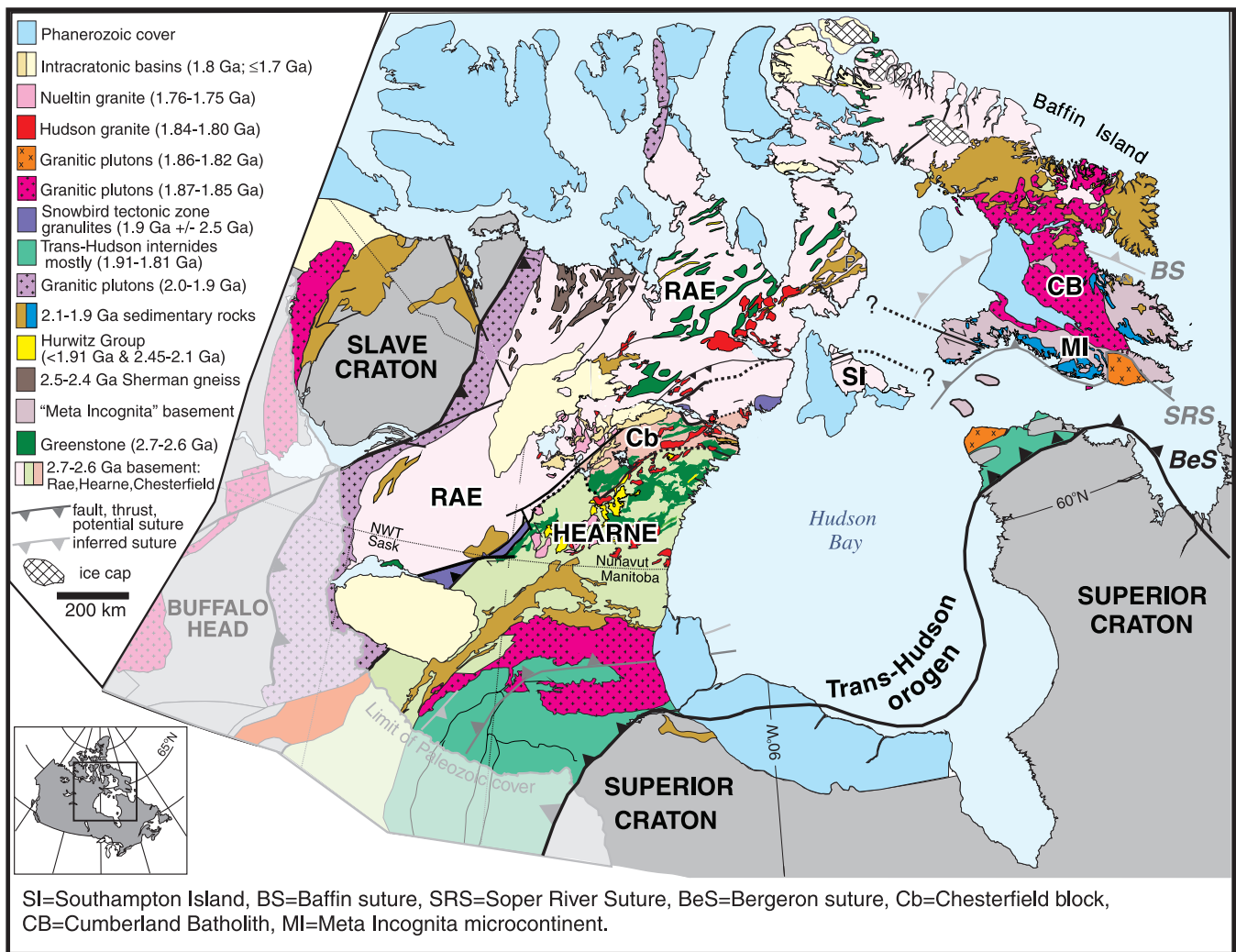


Figure 1. Regional geology of Laurentia flanking Hudson Bay (modified from Berman et al., 2005).

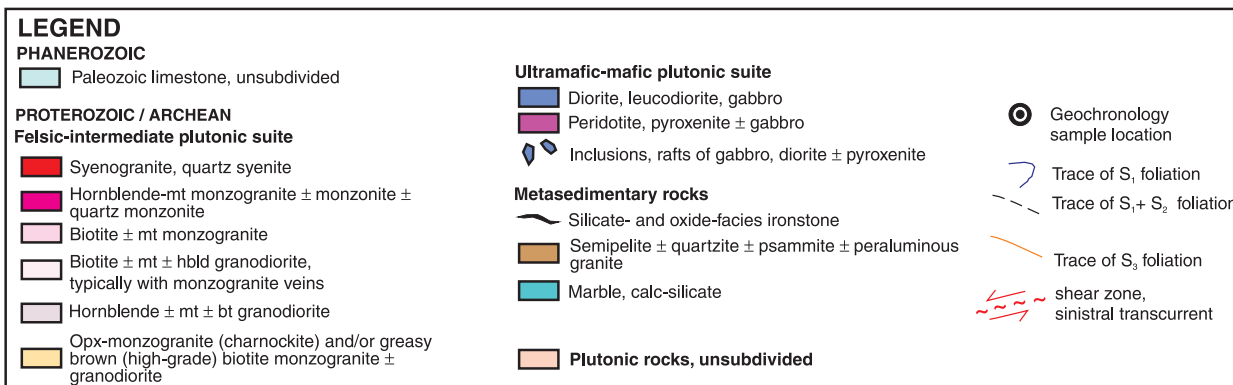
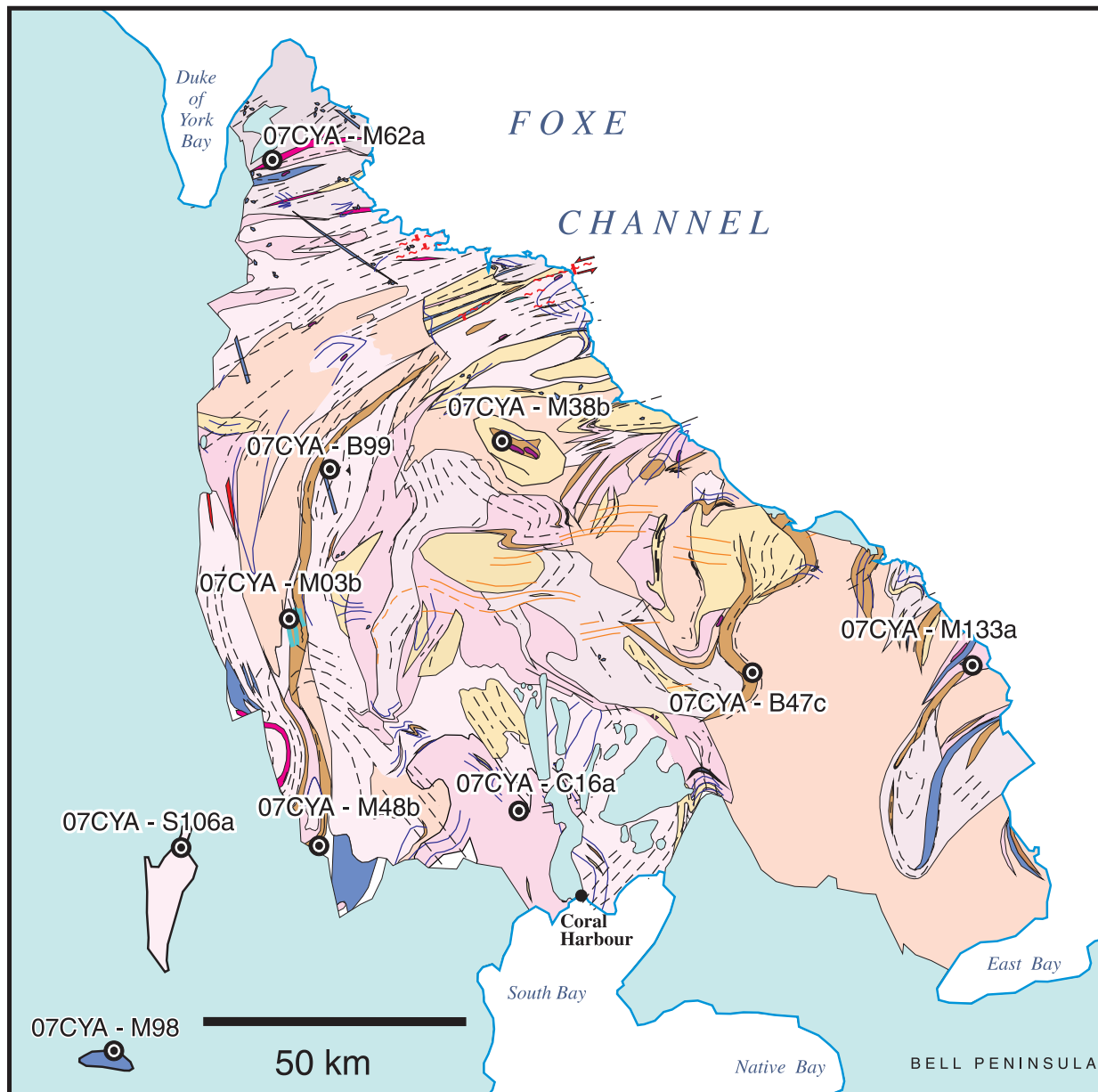


Figure 2. Simplified geological map of study area on Southampton Island.

Although U-Pb ages reveal extensive Paleoproterozoic magmatic (this report) and metamorphic activity (Berman et al., in press), Sm-Nd isotopic data (Whalen et al., in press) indicate Meso- to Paleoproterozoic antiquity to the basement. Geochronological results presented here will help establish the crustal affinity of Southampton Island and aid in the development of a regional framework through comparison with counterparts of the western Churchill Province and eastern Trans-Hudson Orogen.

ANALYTICAL METHODS

Heavy minerals were separated using standard crushing, grinding, and heavy liquid concentration techniques, followed by magnetic sorting of the heavy minerals. Zircons analyzed by ID-TIMS (isotope dilution thermal ionization mass spectrometry) were mechanically abraded prior to analysis (Krogh, 1982). Dissolution in concentrated HF, extraction of U and Pb, and mass spectrometry followed methods described by Parrish et al. (1987) for zircon, and Davis et al. (1997) for rutile. Mass spectrometric data reduction and numerical propagation of analytical uncertainties follow Roddick (1987). ID-TIMS isotopic data are presented in Table 1.

Prior to SHRIMP (sensitive high resolution ion microprobe) analysis, the internal features of the zircons were characterized with backscattered electrons (BSE) or cathodoluminescence (CL) utilizing a Zeiss Evo scanning electron microscope. SHRIMP analytical procedure and U-Pb calibration details are given in Stern (1997) and Stern and Amelin (2003). The analytical work presented here was collected over three sessions on three separate ion probe epoxy mounts under varying instrumental conditions. Specific analytical details for each sample are given in the footnotes of Table 2. Isoplot v. 3.66 (Ludwig, 2003) was used to generate concordia plots and calculate weighted means.

Table 1. ID-TIMS U-Pb results

Fract. ¹	Description ²	Wt. µg	U ppm	Pb ³ ppm	²⁰⁶ Pb/ ²⁰⁴ Pb ⁴	Pb ⁵ pg	Isotopic ratios ⁶						Ages (Ma) ⁸								
							²⁰⁸ Pb/ ²⁰⁶ Pb	²⁰⁷ Pb/ ²³⁵ U	±1σ Abs	²⁰⁶ Pb/ ²³⁸ U	±1σ Abs	Corr. ⁷ coeff.	²⁰⁷ Pb/ ²⁰⁶ Pb	±1σ Abs	²⁰⁶ Pb/ ²³⁸ U	±2σ	²⁰⁷ Pb/ ²⁰⁶ Pb	±2σ	% Disc		
07CYA-B47c (lab # 9424) S-type granite, 64.5048°N 82.69553°W																					
R1 (17)	Clr, Eu, El, Yel, M5	23	138	40	2706	22	0.00	4.337	0.005	0.3010	0.0003	0.9108	0.10451	0.00006	1696.1	2.7	1700.4	2.0	1705.7	2.0	0.64
R2 (12)	Clr, Eu, El, Gr, M5	24	222	64	9204	3	0.00	4.340	0.005	0.3012	0.0003	0.9392	0.10452	0.00005	1697.1	2.7	1701.0	1.9	1705.9	1.6	0.59
R3 (15)	Clr, Eu, El, Gr, M5	27	246	70	2834	44	0.00	4.330	0.005	0.3004	0.0003	0.9142	0.10454	0.00006	1693.3	2.7	1699.1	2.0	1706.2	2.0	0.86
07CYA-S106a (z9426) late monzogranite, 64.7362°N 83.4776°W																					
Z1A (1)	Pr, pBr, fln, M3	1	1673	539	1532	29	0.06	4.914	0.007	0.3210	0.0003	0.8508	0.11101	0.00009	1794.7	2.8	1804.6	2.4	1816.1	2.9	1.35
Z1B (1)	Pr, pBr, fln, M3	3	2246	734	12118	12	0.06	4.971	0.006	0.3242	0.0003	0.9406	0.11121	0.00005	1810.0	2.7	1814.3	1.9	1819.3	1.5	0.59
Z1C (1)	Pr, pBr, fln, M3	3	2334	776	3354	36	0.09	4.914	0.006	0.3210	0.0003	0.9123	0.11104	0.00006	1794.5	2.7	1804.7	2.0	1816.5	1.9	1.39
Z1D (1)	Pr, pBr, fln, M3	5	2405	786	10946	24	0.06	4.974	0.006	0.3243	0.0003	0.9419	0.11123	0.00005	1810.9	2.8	1815.0	1.9	1819.6	1.6	0.55

¹ Sample locations are given relative to the NAD27 datum

² Z=zircon fraction; R=rutile fraction. All zircon fractions are abraded following the method of Krogh (1982). Number in brackets refers to the number of grains in the analysis.

³ Fraction descriptions: Clr=clear, pBr=pale brown, Gr=grey, Yel=yellow, fln=few inclusions, Eu=euhedral, El=elongate, Pr=prismatic, M3=Mag @1.8A 3°SS, M5=Mag @1.8A 5oSS

⁴ Radiogenic Pb

⁵ Measured ratio, corrected for spike and fractionation

⁶ Total common Pb in analysis corrected for fractionation and spike

⁷ Corrected for blank Pb and U and common Pb, errors quoted are 1 sigma absolute; procedural blank values for this study are 0.1pg U and 2 pg Pb for zircon analyses and 10 pg Pb for rutile analyses; Pb blank isotopic composition is based on the analysis of procedural blanks; corrections for common Pb were made using Stacey-Kramers compositions (Stacey and Kramers, 1975).

⁸ Correlation coefficient

⁹ Corrected for blank and common Pb, errors quoted are 2 sigma in Ma

The error on the calibration of the GSC ²⁰⁵Pb-²³¹U-²³⁵U spike utilized in this study is 0.22% (2σ).

All ages quoted in the text are given at the 95% confidence level. Isotopic ratios in Tables 1 and 2 are given at 1σ uncertainty, as are SHRIMP ages. Uncertainties in the ID-TIMS ages are reported in the table at the 2σ level. Error ellipses on Concordia diagrams (Fig. 3–12) are plotted at the 2σ uncertainty level.

U-PB RESULTS

07CYA-M62a (lab # z9427) hornblende monzogranite

A hornblende-biotite monzogranite unit was collected north of the prominent east-west shear zone from the north part of the island (Fig. 2). It is characterized by abundant mafic and ultramafic xenoliths, and locally contains xenoliths of metasedimentary rocks, and biotite-magnetite±orthopyroxene granodiorite. It was metamorphosed to amphibolite facies and is intensely intruded by pink-weathering monzogranite veins. The majority of recovered zircons are prismatic and of varying quality, whereas a secondary population of zircons are clear, colourless, high-quality equant grains. In BSE images the majority of prismatic and equant zircons are concentrically zoned, many with unzoned overgrowths. The pattern of ages observed in these grains corresponds with morphological, zoning, and chemical characteristics. As single-component grains or cores, prismatic and equant zoned zircons typically have low to moderate U concentrations (52–352 ppm U) and moderate Th/U ratios (0.3–0.9). The eleven oldest zoned zircons yielded a weighted mean ²⁰⁷Pb/²⁰⁶Pb age of 2692 ± 6 Ma (MSWD=1.12, probability=0.34), which is interpreted as the monzogranite crystallization age (Fig. 3). Rare, unzoned anhedral and equant zircons with low to moderate U content (52–678 ppm) and low Th/U (0.01–0.02) yield a weighted mean ²⁰⁷Pb/²⁰⁶Pb age of 1884 ± 14 (n=5, MSWD=0.75,

07CYA-M62a hornblende monzogranite

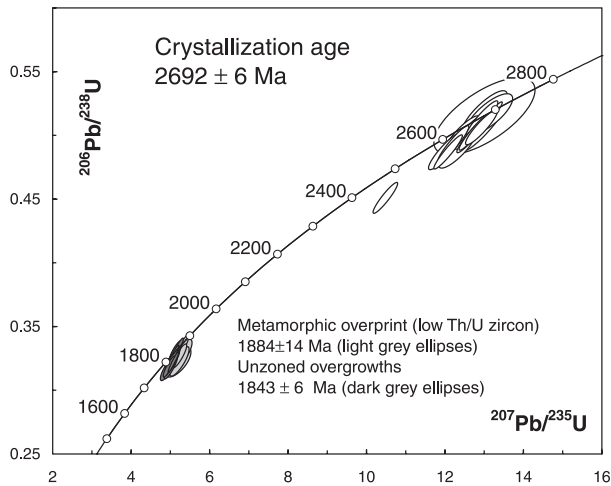


Figure 3. Concordia diagram for sample 07CYA-M62a. Magmatic zircons are shown as unfilled ellipses, metamorphic zircons are shown in shades of grey.

07CYA-B47c S-type granite

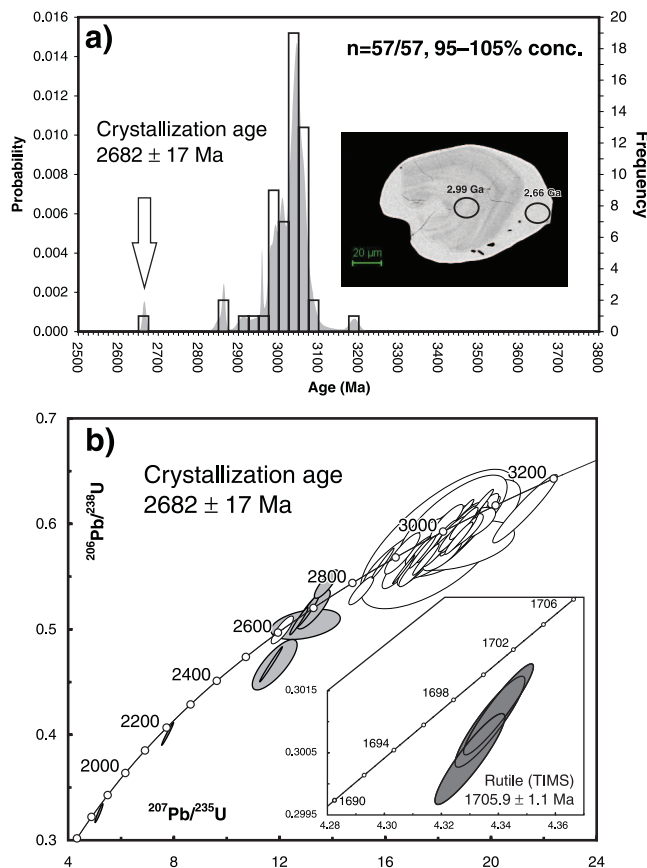


Figure 4. a) Probability density diagram illustrating the distribution of inherited zircon ages as well as the magmatic age for sample 07CYA-B47c. b) Corresponding concordia diagram. Inherited zircons are shown as unfilled ellipses, magmatic overgrowths are shown in light grey, and dark grey ellipses record later metamorphic overprint. ID-TIMS results for rutile shown in inset.

probability=0.56). Unzoned rims surrounding ca. 2.7 Ga and 1.88 Ga cores yield a weighted mean $^{207}\text{Pb}/^{206}\text{Pb}$ age of 1843 ± 6 Ma ($n=15$ analyses from 14 zircons, $\text{MSWD}=1.6$, probability=0.07). The two younger ages likely reflect an earlier metamorphic episode (ca. 1.88 Ga) and the intrusion of voluminous felsic magma (ca. 1.84 Ga).

07CYA-B47c (z9424) S-type granite

An enclave of psammite-semipelite exposed on eastern central part of the island is cut by garnet-muscovite granite interpreted as representing a crustal melt, possibly derived from the metasediments (Fig. 2). A sample of the granite was collected to constrain the timing of crustal melting and provide a minimum age for the sedimentary rocks cut by the granite. Zircons are typically clear, colourless and sub-hedral to prismatic. In BSE images, oscillatory zoning is observed in most grains and many exhibit unzoned, bright in BSE (high U) rims ranging in thickness from 5 to 20 μm (Fig. 4a inset). Oscillatory zoned zircon yields dates ranging from 2854 to 3190 Ma, with a dominant mode at 3.05 Ga and a subordinate one at 3.00 Ga (Fig. 4a), all interpreted as inherited. Analyses of seven unzoned high-U rims yielded a Tukey's biweight mean (Hoaglin et al., 1983) $^{207}\text{Pb}/^{206}\text{Pb}$ age of 2682 ± 17 Ma, interpreted as the time of crustal melting and emplacement/crystallization of the S-type granite (Fig. 4b). One zircon yielded younger non-reproducible dates of 2224 and 1867 Ma, however, this grain is not interpreted as an original component of the S-type granite. Paleoproterozoic magmatic overprints are common on Southampton Island and spurious younger ages appear to reflect Pb-loss or the inadvertent inclusion of secondary magmatic phases during sampling. The age of 2682 ± 17 Ma for the S-type granite indicates an episode of crustal melting in the Archean and provides a minimum age of the psammite-semipelite sequence.

Three multi-grain rutile fractions were analyzed by TIMS in order to constrain a cooling age for the S-type granite (Table 1). All three fractions gave statistically identical ages of 1705.9 ± 1.0 Ma ($\text{MSWD}=0.064$, probability=0.94), the time of final cooling through ca. 420°C, a field-based estimate of the rutile closure temperature in slowly cooled terranes (Mezger et al. 1989; see Fig. 4b inset).

07CYA-M03b (z9421) quartzite

A sample of quartzite, 07CYA-M03b, was taken from the western margin of the exposed basement, where narrow panels of quartzite and calc-silicate are aligned with the dominant north-south fabric (Fig. 2). The ages of detrital zircons provide insight into the provenance of this quartzite-carbonate association and constrain the maximum age of deposition. The zircons are highly variable, and range from clear, colourless prisms to brown, highly fractured grains. Most are euhedral to subhedral with slightly resorbed facets; none exhibit strong mechanical abrasion suggestive of

Table 2. (cont.)

Spot name	U (ppm)	Th (ppm)	Th/U	Pb* (ppm)	206Pb/208Pb	207Pb/208Pb	f(206)208	206Pb/208Pb	207Pb/208Pb	206Pb/238U	207Pb/238U	206Pb/235U	207Pb/235U	Apparent ages (Ma)				Disc. (%)						
														±206Pb/208Pb	±207Pb/208Pb	±206Pb/238U	±207Pb/238U							
9422-43.1	69	58	0.87	29	1	5.89E-05	5.87E-05	0.0010	0.2480	0.0070	6.331	0.125	0.3525	0.0048	0.7737	0.1302	0.0017	1947	23	2023	18	2101	22	7.4
9422-88.2	93	47	0.52	36	1	1.93E-05	6.38E-05	0.0003	0.1556	0.0050	6.373	0.132	0.3510	0.0046	0.7237	0.1316	0.0019	1940	22	2029	17	2120	25	8.5
9422-218.3	131	95	0.74	56	3	8.59E-05	5.51E-05	0.0015	0.2383	0.0043	6.675	0.128	0.3580	0.0052	0.8310	0.1352	0.0015	1973	25	2069	17	2167	19	9
9422-92.2	78	30	0.40	29	0	1.49E-05	6.11E-05	0.0003	0.1100	0.0040	6.605	0.136	0.3516	0.0055	0.8316	0.1362	0.0016	1942	26	2060	18	2180	20	10.9
9422-218.6	154	122	0.81	65	4	8.53E-05	3.14E-05	0.0015	0.2476	0.0080	6.670	0.106	0.3511	0.0049	0.9298	0.1378	0.0008	1940	24	2069	14	2200	10	11.8
9422-22.1	109	50	0.48	44	0	1.00E-05	1.00E-05	0.0002	0.1371	0.0028	7.150	0.110	0.3698	0.0043	0.8255	0.1402	0.0012	2028	20	2130	14	2230	15	9
9422-47.3	131	106	0.84	59	0	1.00E-05	1.00E-05	0.0004	0.2600	0.0040	7.242	0.129	0.3731	0.0049	0.8096	0.1408	0.0015	2044	23	2142	16	2237	8	8.6
9422-50.1	263	465	1.83	146	2	2.02E-05	1.21E-05	0.0004	0.5439	0.0039	7.642	0.096	0.3814	0.0042	0.9298	0.1453	0.0007	2083	20	2190	11	2292	8	9.1
9422-30.1	112	115	1.05	51	1	4.05E-05	3.14E-05	0.0007	0.3074	0.0101	7.352	0.321	0.3660	0.0110	0.7673	0.1457	0.0041	2010	52	2155	40	2296	49	12.4
9422-13.1	86	74	0.89	41	1	2.50E-05	5.89E-05	0.0004	0.2576	0.0046	8.106	0.150	0.3954	0.0045	0.6987	0.1481	0.0020	2148	21	2243	17	2331	23	7.9
9422-28.1	41	46	1.15	20	1	3.80E-05	1.00E-04	0.0007	0.3128	0.0094	7.904	0.192	0.3821	0.0049	0.6230	0.1507	0.0029	2086	23	2220	22	2346	33	11.1
9422-34.1	82	71	0.90	39	2	7.53E-05	8.01E-05	0.0013	0.2787	0.0051	8.028	0.165	0.3856	0.0051	0.7277	0.1510	0.0021	2102	24	2234	19	2357	24	10.8
9422-36.1	79	58	0.75	36	1	2.89E-05	6.39E-05	0.0005	0.2202	0.0051	8.229	0.172	0.3875	0.0062	0.8377	0.1540	0.0018	2111	29	2257	19	2391	20	11.7
9422-48.2	162	148	0.94	80	2	4.19E-05	2.04E-05	0.0007	0.2738	0.0059	8.632	0.121	0.4002	0.0048	0.9054	0.1564	0.0009	2170	22	2300	13	2417	10	10.2
9422-4.1	77	41	0.55	35	1	5.08E-05	3.14E-05	0.0009	0.1616	0.0038	8.737	0.133	0.3997	0.0051	0.8892	0.1586	0.0011	2167	23	2311	14	2440	12	11.2
9422-11.1	138	77	0.57	61	0	1.00E-05	1.00E-05	0.0002	0.1657	0.0039	8.608	0.277	0.3875	0.0083	0.7459	0.1611	0.0035	2111	38	2297	30	2467	37	14.4
9422-5.1	199	293	1.52	113	2	2.90E-05	1.82E-05	0.0005	0.4504	0.0046	9.154	0.124	0.4100	0.0050	0.9377	0.1619	0.0008	2215	23	2353	12	2476	8	10.5
9422-48.1	87	80	0.94	42	3	9.52E-05	6.21E-05	0.0017	0.2704	0.0045	8.904	0.162	0.3954	0.0055	0.8370	0.1633	0.0016	2148	26	2328	17	2490	17	13.8
9422-2.1	46	24	0.53	21	0	1.00E-05	1.00E-05	0.0002	0.1657	0.0075	9.138	0.206	0.4029	0.0060	0.7414	0.1645	0.0025	2183	27	2352	21	2502	26	12.8
9422-92.1	30	18	0.63	15	3	2.35E-04	2.08E-04	0.0041	0.1747	0.0124	9.794	0.327	0.4291	0.0072	0.6016	0.1656	0.0045	2301	32	2416	31	2513	46	8.4
9422-15.1	33	33	1.04	17	1	1.03E-04	8.88E-05	0.0018	0.2935	0.0141	9.859	0.251	0.4166	0.0060	0.6583	0.1716	0.0033	2245	27	2422	24	2574	33	12.8
9422-12.1	113	99	0.91	61	2	4.86E-05	2.90E-05	0.0008	0.2701	0.0066	10.267	0.143	0.4330	0.0050	0.8916	0.1720	0.0011	2319	23	2459	13	2577	11	10
9422-218.2	91	62	0.70	47	0	4.20E-05	3.59E-05	0.0001	0.2012	0.0066	10.645	0.183	0.4384	0.0054	0.8000	0.1773	0.0019	2330	24	2493	16	2628	17	11.4
9422-8.1	79	28	0.36	39	0	1.00E-05	1.00E-05	0.0002	0.1103	0.0026	11.348	0.163	0.4469	0.0052	0.8650	0.1842	0.0013	2381	23	2552	14	2691	12	11.5
9422-218.5	68	45	0.69	43	3	8.33E-05	6.17E-05	0.0014	0.1855	0.0091	15.619	0.369	0.5226	0.0081	0.8141	0.2168	0.0030	2710	39	2854	23	2957	22	8.3
9422-218.4	140	157	1.16	99	4	5.91E-05	2.63E-05	0.0010	0.3115	0.0076	16.299	0.302	0.5385	0.0082	0.8835	0.2195	0.0019	2777	35	2895	18	2977	14	6.7
9422-218.1	126	135	1.11	94	0	8.00E-06	3.02E-05	0.0001	0.3011	0.0049	17.555	0.256	0.5700	0.0068	0.8797	0.2234	0.0016	2908	28	2966	14	3005	11	3.2

Analytical details: mount: IP48.1, 23 µm spot size, primary beam intensity 6-7 nA, 6 scans
 Error in 206Pb/238U calibration: 1.0%
 207Pb/206Pb ages given: *in italics* were used to calculate the weighted mean age given in the text.
07CYA-C16a (lab# z9557) birimigranodiorite 64.27769 N 83.4888 W
 Spot name follows the convention x.y.z; where x = grain number, y = grain number and z = spot number. Multiple analyses in an individual spot are labelled as x.y.z.
 Uncertainties reported at 1σ (absolute) and are calculated by numerical propagation of all known sources of error.
 * refers to radiogenic Pb (corrected for common Pb), calculated using the 204Pb-method; common Pb composition used is the surface blank (4/6.0.05770; 7/6.0.89500; 8/6.2.13840)
 † refers to radiogenic Pb (corrected for common Pb), calculated using the 204Pb-method; common Pb composition used is the surface blank (4/6.0.05770; 7/6.0.89500; 8/6.2.13840)
 Discrepancy relative to origin = 100 * (1-(206Pb/238U age)/(207Pb/206Pb age))
 Calibration standard 6266: U = 910 ppm; Age = 559 Ma; 206Pb/238U = 0.09059
 Th/U calibration: F = 0.039001UO + 0.85600
 The notes above apply to all data in Table 2.
 Notes (see Stern, 1997):
 Sample locations are given relative to the NAD27 datum.
 Spot name follows the convention x.y.z; where x = grain number, y = grain number and z = spot number. Multiple analyses in an individual spot are labelled as x.y.z.
 Uncertainties reported at 1σ (absolute) and are calculated by numerical propagation of all known sources of error.
 * refers to radiogenic Pb (corrected for common Pb), calculated using the 204Pb-method; common Pb composition used is the surface blank (4/6.0.05770; 7/6.0.89500; 8/6.2.13840)
 † refers to radiogenic Pb (corrected for common Pb), calculated using the 204Pb-method; common Pb composition used is the surface blank (4/6.0.05770; 7/6.0.89500; 8/6.2.13840)
 Discrepancy relative to origin = 100 * (1-(206Pb/238U age)/(207Pb/206Pb age))
 Calibration standard 6266: U = 910 ppm; Age = 559 Ma; 206Pb/238U = 0.09059
 Th/U calibration: F = 0.039001UO + 0.85600
 The notes above apply to all data in Table 2.

sedimentary transport across long distances (Fig. 5a inset). In BSE, most zircons exhibit oscillatory zoning, although some grains are unzoned. Sixty-four analyses, carried out on 55 separate zircon grains, yield $^{207}\text{Pb}/^{206}\text{Pb}$ ages between 1823 and 3255 Ma (Fig. 5a). Paleoproterozoic ages were obtained from a distinct tip on grain 104 and an equant, unzoned zircon (grain 22). These zircons are not interpreted as detrital, rather as representing geological contamination from the pervasive Paleoproterozoic plutonism in the area (*see* results for plutonic samples below). Interpreted detrital age distributions are highlighted in the probability density diagram (Fig. 5b), with the majority of results between 2.68 Ga and 2.95 Ga and prominent modes at 2.7 Ga, 2.82 Ga, and 2.91 Ga. The youngest detrital zircon yielded a weighted

mean $^{207}\text{Pb}/^{206}\text{Pb}$ age of 2615 ± 23 Ma ($n=3$, $\text{MSWD}=2.9$, probability of fit=0.06). A fourth high U replicate analysis was excluded from the calculation of the mean and the remaining excess scatter may also be the result of minor Pb loss. As such, 2615 ± 23 Ma is considered the minimum age for the youngest detrital zircon, and a maximum age of deposition. This dataset does not confirm if the quartzite/calc-silicate sequence on Southampton Island was deposited during the late Archean or during the Paleoproterozoic (i.e., time equivalent to Paleoproterozoic Amer and Ketyet River groups; Rainbird et al., 2010). It does, however, effectively distinguish the quartzite-carbonate sequence from the psammite-semipelite sequence described earlier, which was deposited prior to 2682 ± 17 Ma.

07CYA-M48b (z9548) aphanitic epiclastic rock

A distinctive, grey, aphanitic, strongly foliated, folded and quartz-veined unit associated with quartzose wacke in the southwest corner of the exposed basement (Fig. 2) was considered the best candidate for an intermediate metavolcanic rock on Southampton Island. Subsequent examination of zircon morphology and evaluation of the consistency of ages has revised this interpretation to an epiclastic origin. Zircons recovered from the sample are highly variable in colour and morphology, ranging from clear and colourless to dark brown and turbid. Most grains are prismatic to stubby, ranging from well-faceted to well-rounded (Fig. 6a inset). The recovery of rounded and frosted zircon implies some degree of sedimentary transport. Oscillatory zoning is visible in brown zircons in both plane light and in BSE images, whereas the colourless grains are typically unzoned in plane light but may exhibit faint concentric zoning in BSE images. The $^{207}\text{Pb}/^{206}\text{Pb}$ age profile is dominated by 2.60 and 2.62 Ga dates with sporadic results between 2.70 Ga and 3.17 Ga (Fig. 6b). The dominant mode at ca 2.61 Ga is a composite population of minor ca. 2.60 Ga zircon and more prevalent 2.62 Ga ages. A metamorphic overprint is observed in high U, low Th/U overgrowths with ages between 1815 and 1764 Ma (Fig. 6a). Further evidence for late disturbance of the isotopic systematics is provided by non-reproducible replicate analyses within the same zircon domain (*see* analyses of grains 17, 76, 89, Table 2). The youngest detrital zircon yields two replicate analyses with a mean age of 2578 ± 9 Ma; however, this grain is of poor quality, and considering that Pb-loss is documented in other grains, this age may underestimate the maximum age of deposition. A more conservative age estimate for the youngest detrital zircon is 2599 ± 15 Ma ($\text{MSWD}=2.7$, probability=0.042) constrained by the four oldest replicate analyses of grain 49. The provenance profile for this sample differs substantially from that of 07-CYA-M03b, although both constrain maximum ages of deposition to be late Archean.

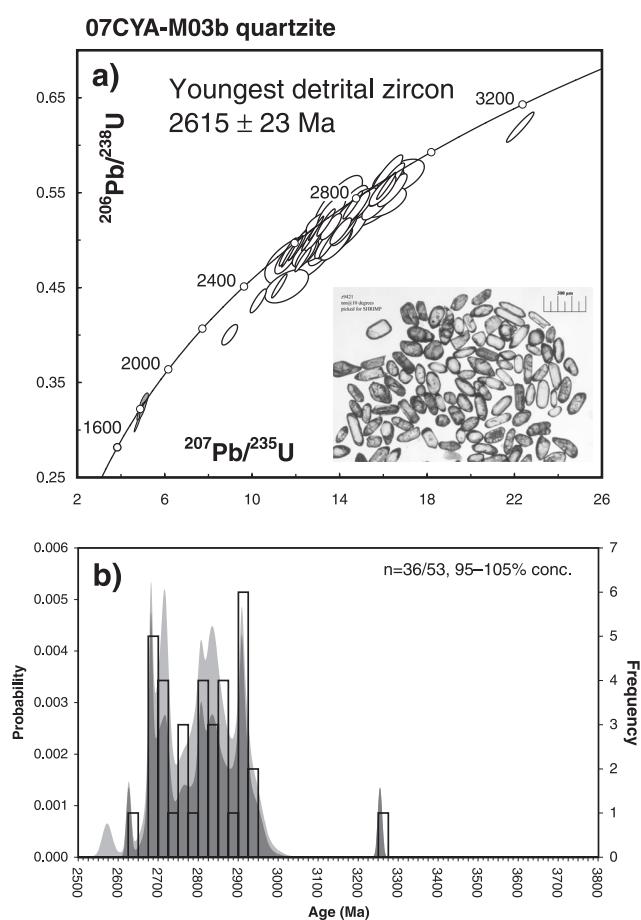


Figure 5. a) Concordia diagram for sample 07CYA-M03b. Detrital zircon results are shown as unfilled ellipses, grey ellipses record later overprint. Scale bar on inset photo is 300µm. **b)** Probability density diagram illustrating the distribution of detrital age results. The dark grey curve and histogram represent data within 5% of concordance ($n=36$); the light grey curve illustrates all data regardless of concordance ($n=53$). Replicate analyses are not plotted.

07CYA-M48b
fine-grained volcani(?)clastic

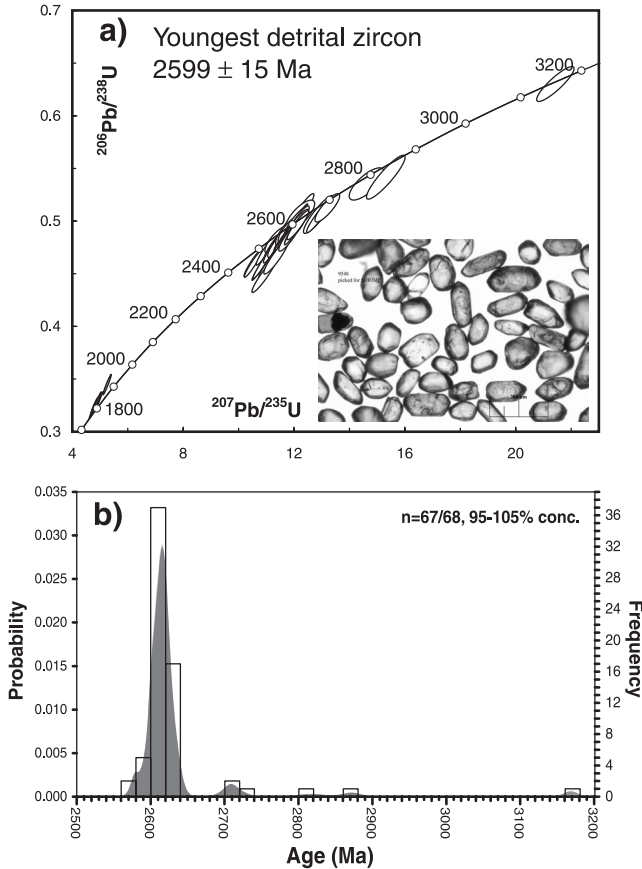


Figure 6. a) Concordia diagram for sample 07CYA-M48b. Detrital zircon results are shown as unfilled ellipses; grey ellipses record later overprint. b) Probability density diagram illustrating the distribution of detrital age results. The dark grey curve and histogram represent data within 5% of concordance ($n=67$); the light grey curve illustrates all data regardless of concordance ($n=68$). Replicate analyses are not plotted.

07CYA-M98 (z9425) quartz porphyry tonalite

A distinctive blue quartz porphyry of intermediate composition collected from an inlier in the southwest corner of the map area (Fig. 2) intrudes locally retrogressed mafic granulites. Felsic granitic rocks, regionally pervasive elsewhere, are notably absent in this inlier such that retrogression of the mafic granulites is attributed to the intrusive porphyritic phase. Zircons recovered from this sample are largely clear, colourless, high-quality, subhedral, equant prisms with a smaller proportion of light brown, highly fractured prisms. Twenty-seven analyses were carried out on twenty-two zircon grains. A weighted mean $^{207}\text{Pb}/^{206}\text{Pb}$ age of 1934 ± 8 Ma ($n=19$, $\text{MSWD}=0.42$, $\text{probability}=0.98$) is interpreted as the crystallization age of the porphyry (Fig. 7). In the case of grains with replicate analyses, only the oldest replicate was included in the mean, since multiple

07CYA-M98 quartz porphyry tonalite

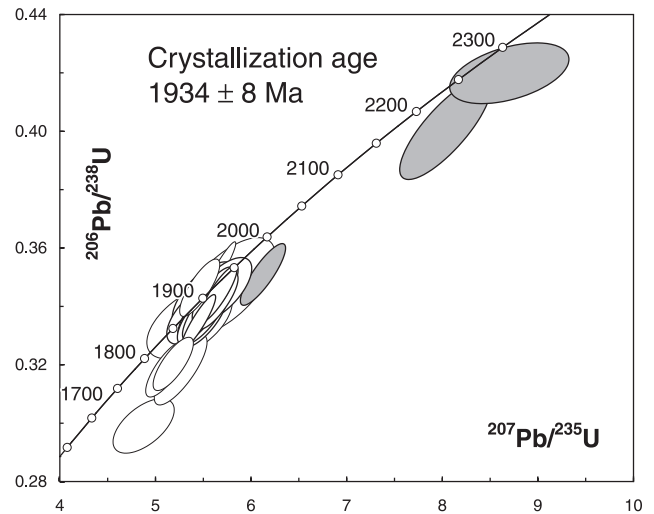


Figure 7. Concordia diagram for sample 07CYA-M98. Magmatic zircons are shown as unfilled ellipses; inherited zircons are shown in shades of grey.

analyses from other individual grains (grain 2, 26, 54) were not reproducible. Three zircons belonging to the subordinate group of poor-quality zircon gave older ages of between 2050 and 2351 Ma. All three results are 4–6% discordant and are considered minimum ages of inheritance. Given that the porphyry retrogresses the host mafic granulite rocks, its crystallization age of 1934 ± 8 Ma not only provides a minimum age for a mafic plutonic event at this locality, but also provides a minimum age on a high-grade metamorphic event that affected this region.

07CYA-B99 (z9423) biotite-orthopyroxene granodiorite

This sample of bi±opx granodiorite appears representative of regionally extensive granulite facies plutonic rocks exposed on Southampton Island. It was collected in the western part of the exposed basement characterized by a dominant north-south fabric (Fig. 2). Close to the sampling site, the opx-bearing granodiorite is flooded with pink weathering, non-granulite facies monzogranite. In order to minimize contamination through sampling, a homogenous 40 cm wide layer was targeted for geochronology. Recovered zircons are highly variable, and include a population of clear, colourless prisms with multi-faceted or resorbed faces, and a second population of fractured and oscillatory zoned, pale brown, elongate prisms. Wide, pale brown overgrowths are noted in plane light, however these are rare. In BSE images the overgrowths are relatively bright, indicating elevated U concentrations. A second generation of overgrowth is also apparent in BSE images, and is characterized by lower U content. Oscillatory zoned zircons, both as cores or single-component grains, yield a range of Archean ages between 2.65 and 3.68 Ga that are interpreted as inherited. The dominant inherited component

is Eoarchean, 3.63 to 3.66 Ga (Fig 8a, Table 2). A second population of low U (17–397 ppm), and very low Th (1–2 ppm) unzoned zircons yields a mean $^{207}\text{Pb}/^{206}\text{Pb}$ age of 1931 ± 19 Ma (Tukey’s Biweight mean) from 18 analyses of 11 zircon grains (Fig. 8b). Three replicate analyses of a grain with similar chemistry yield distinctly older ages (2087 Ma and 2150 Ma) and are not included in the calculation of the mean. High U (2142–2772 ppm) zircon overgrowths yield a weighted mean $^{207}\text{Pb}/^{206}\text{Pb}$ age of 1860 ± 4 Ma ($n=5$, $\text{MSWD}=1.7$, $\text{probability}=0.15$). Moderate U (122–567 ppm) zircon overgrowths and rare, single-component grains have distinctly higher Th/U (0.6–2.6, most greater than 1) that yield a weighted mean $^{207}\text{Pb}/^{206}\text{Pb}$ age of 1840 ± 7 Ma ($n=11$, $\text{MSWD}=0.14$, $\text{probability}=0.999$).

Although the isotopic data from this sample highlight several significant ages, 1931 ± 19 Ma is the preferred crystallization age of the bi + opx granodiorite as it is consistent with the fact that this rock contains S_1 , determined to have

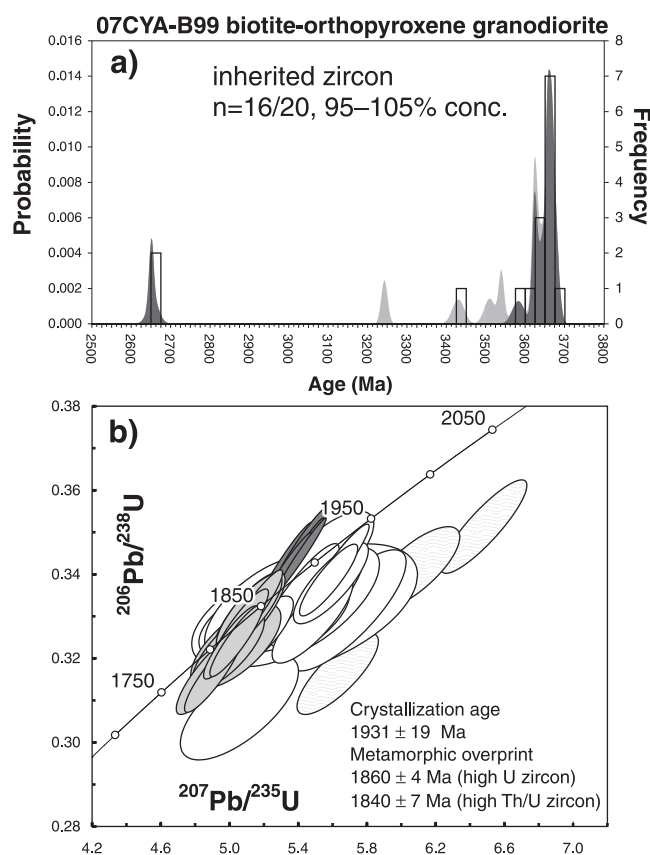


Figure 8. a) Probability density diagram illustrating the distribution of inherited zircon ages for sample 07CYA-B99. The dark grey curve and histogram represent data within 5% concordance ($n=16$); the light grey curve illustrates all data regardless of concordance ($n=20$). **b)** Concordia diagram illustrating Paleoproterozoic ages only. Low U, Th, magmatic zircons are shown as unfilled ellipses. Three zircons of similar chemistry that were not included in the calculation of the mean are shown by the striped pattern. Two generations of overgrowths are shown as dark grey (high U zircon) and light grey (moderate U, Th, high Th/U zircon) ellipses.

developed at ca. 1.88 Ga (Berman et al., in press) and F_2 folds (dated at 1.86–1.84 Ga). Overgrowth ages younger than 1880 Ma in this sample are interpreted as reflecting the influence of a pervasive Paleoproterozoic thermo-magmatic event(s), as recorded by the ubiquitous pink granitic veins that cut the unit.

07CYA-M38b (z9422) gabbroic anorthosite

Gabbroic anorthosite forms a minor component of a layered ultramafic complex exposed on northeastern Southampton Island (Fig. 2). The presence of garnet + orthopyroxene + clinopyroxene reflects attainment of granulite facies conditions (Yakymchuk et al., 2008). Elsewhere on the island, mafic-ultramafic units are spatially associated with metasedimentary units and are commonly observed as enclaves and inclusions within intermediate to felsic plutonic units, suggesting that mafic-ultramafic plutonism postdates the supracrustal rocks and predates granitoid emplacement. Zircons recovered from the gabbroic anorthosite are typically clear and colourless. Grains may be anhedral or equant, the former characterized by abundant quartz and plagioclase inclusions sub-1 μm to 10 μm in diameter, and the latter with few inclusions or fractures. Equant zircons exhibit relatively straightforward sector zoning in CL images (Fig. 9 inset top left). Anhedral grains typically have poor CL response (dark) and are variably “speckled” with bright CL domains (Fig. 9 inset). This unusual inner structure is broadly similar to features documented in zircon recovered from granulite-grade rocks elsewhere (Corfu et al., 2003; Bröcker and Enders, 1999). The weighted mean $^{207}\text{Pb}/^{206}\text{Pb}$ age of twenty analyses of twelve sector-zoned grains is 1870 ± 10 Ma ($\text{MSWD}=1.2$, $\text{probability}=0.21$,

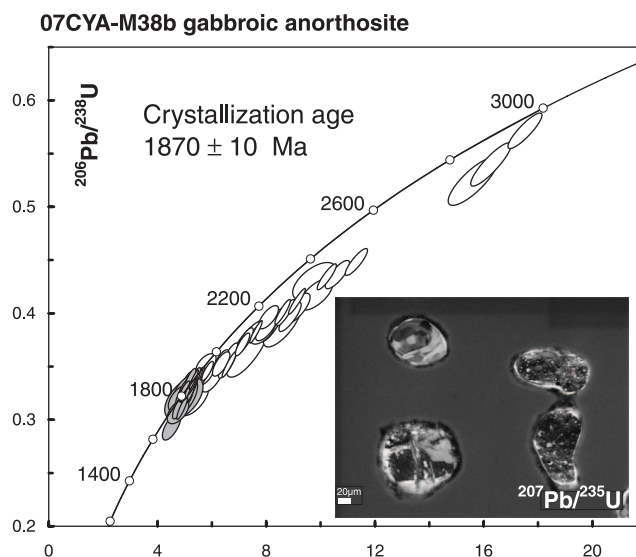


Figure 9. Concordia diagram for sample 07CYA-M38b. Sector-zoned zircons are shown as grey ellipses; speckled zircons are unfilled. Inset presents a CL image of typical zircons illustrating the two dominant textures (top left: sector-zoned zircon, remaining three: speckled zircon).

Fig. 9). Speckled zircons yield discordant $^{207}\text{Pb}/^{206}\text{Pb}$ ages between 1820 ± 44 Ma (2μ) to 2577 ± 22 Ma (2σ) aligned with an upper intercept of ca. 3.0 Ga. Grain 21a comprises an oscillatory zoned inner region and a speckled outer region separated by diffuse boundaries. The oldest, most concordant analysis from this grain constrains the upper intercept at 3005 ± 22 Ma with younger, more discordant analyses along the same chord as the bulk of the data (see Table 2).

Peak metamorphic conditions of 850–900°C and 0.9–1.0 GPa were determined from an opx-cpx-plag assemblage within garnet from the mafic granulite complex (Yakymchuk et al., 2008), and the preservation of garnet mantled by plag-opx-spinel symplectite provides a record of exhumation and decompression. Consideration of the geochronological data suggests two main scenarios: emplacement at ca. 3.0 Ga with subsequent burial to granulite facies conditions at 1870 ± 10 Ma, or intrusion of the ultramafic complex at 1870 ± 10 Ma at a deep crustal level (granulite facies stability). The texture and isotopic systematics of the zircon in this sample provide some insight into the preferred scenario. The unique speckled appearance and strongly disturbed isotopic systematics of the older zircons are not typical of rocks that reach granulite facies conditions through slow burial or tectonic thickening (i.e. opx-granodiorite 07CYA-B99). Rather, we suggest these are xenocrystic in origin and strongly disturbed by exceptional conditions, such as interaction with the ultra-high temperatures of a mafic magma (ca 1200°C, Wyllie, 1981) and prolonged residence in the elevated thermal regime of the deep crust. Accordingly, our preferred interpretation is intrusion of ultramafic magma at 1870 ± 10 Ma at depth into crust with Mesoproterozoic ancestry.

07CYA-C16a (z9557) biotite-magnetite granodiorite

A sample of pink weathering, regionally extensive, biotite-magnetite granodiorite, bearing no evidence of attainment of granulite facies metamorphism, was collected from the south-central part of the exposed Precambrian basement (Fig. 2). This unit cuts metasedimentary and mafic lithologies and contains a strong D_2 fabric. It is inferred to correlate with the pervasive, cm-wide, pink-weathering granodiorite veins that are ubiquitous and cut granulite-facies felsic plutonic rocks. Recovered zircons are prismatic to equant, with well-developed facets reflecting minor resorption. In plane light, oscillatory zoning is apparent in pale brown grains but not in the colourless variety. Most grains exhibit broad, concentric zoning patterns that are visible in BSE images. Results are variably discordant, with $^{207}\text{Pb}/^{206}\text{Pb}$ ages between 2458 Ma and 2712 Ma from pale brown zircons with moderate to high U, and interpreted as minimum inheritance ages (Fig. 10). A subset of clear, colourless, prismatic zircon yield a weighted mean $^{207}\text{Pb}/^{206}\text{Pb}$ age of 1852 ± 8 Ma ($n=18$, MSWD=1.2, probability=0.22), the interpreted crystallization age of the

granodiorite (Fig. 10). In addition, ten younger analyses yield dates between 1825 Ma and 1777 Ma. These younger ages are interpreted as being the result of Pb-loss from igneous zircon grains given their non-reproducibility within the same internal zircon zonation domain. The crystallization age for this S_2 foliated biotite granodiorite provides a maximum age of penetrative D_2 strain.

07CYA-M133a (z9558) quartz diorite

Quartz diorite forms a prominent ridge on the east coast of the island, south of Cape Fisher (Fig. 2), and occurs as mafic enclaves in surrounding monzogranite-granodiorite, becoming more abundant with increasing proximity to the ridge. The quartz diorite ridge exhibits a well-developed fabric parallel to S_2 . Accordingly, the age of this diorite provides insight into mafic plutonic activity in this region and a maximum age for the onset of D_2 . Zircons recovered from the quartz diorite are fragmental to anhedral or equant, and pale brown to colourless. Six analyses of pale brown fragmental or anhedral zircons yield discordant $^{207}\text{Pb}/^{206}\text{Pb}$ ages between 2332 Ma and 2511 Ma. The results fall on a chord suggesting Pb-loss from zircons of a single age, with the oldest $^{207}\text{Pb}/^{206}\text{Pb}$ age (i.e., ca. 2511 Ma) representing the minimum age of inherited material in the diorite (Fig. 11). The remaining 19 analyses, from both pale brown, fragmental zircon and colourless, equant zircon yield a weighted mean $^{207}\text{Pb}/^{206}\text{Pb}$ age of 1842 ± 5 Ma (MSWD=1.12, probability of fit=0.33), interpreted as the crystallization age (Fig. 11). This age highlights a third, separate, younger mafic plutonic event and establishes that penetrative D_2 strain affected this part of the island after ca. 1842 ± 5 Ma.

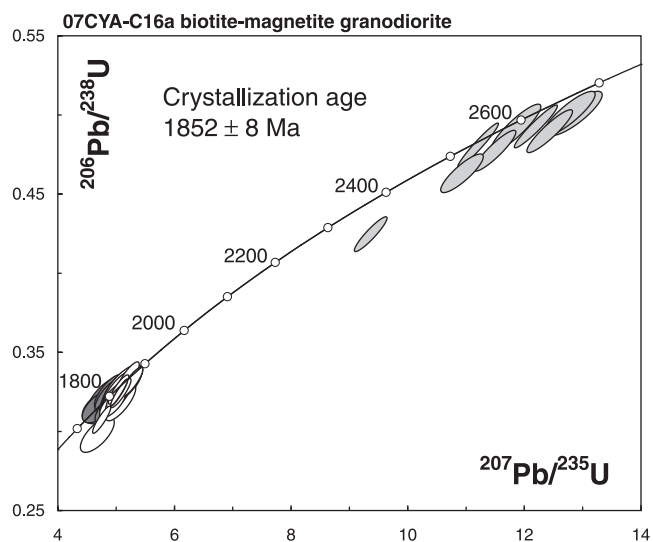


Figure 10. Concordia diagram for sample 07CYA-C16a. Magmatic zircons are shown as unfilled ellipses; inherited zircons are shown in light grey. Analyses not included in the calculation of the weighted mean are shown in dark grey.

07CYA-S106a (z9426) late syenogranite

Undeformed syenogranite collected from a basement inlier 25 km west of the main Precambrian highland (Fig. 2), represents a plutonic phase that has not sustained penetrative deformation recorded by the other samples across Southampton Island described earlier. A homogeneous population of moderate quality, pale brown prisms with few inclusions or fractures was deemed suitable for ID-TIMS analyses. Four single fractions were submitted and the results are presented in Table 1 and Figure 12. The fractions are 0.6% and 1.4% discordant and contain 1600–2400 ppm U. They yield an upper intercept age of 1821.7 ± 2.5 Ma (MSWD=0.09, probability of fit=0.92) interpreted as the

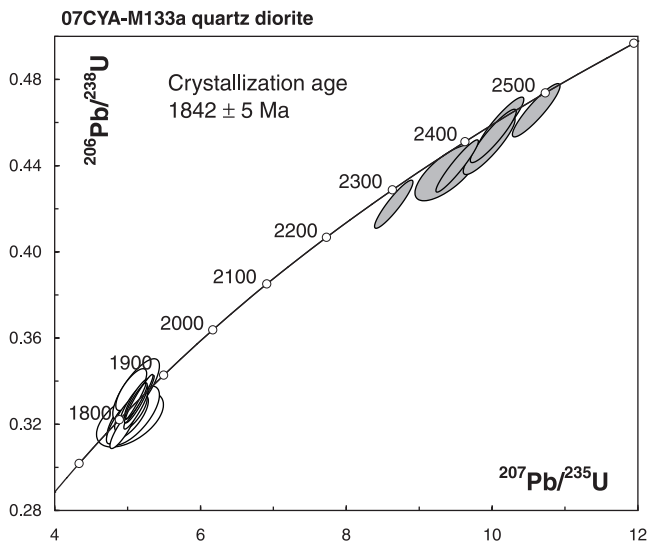


Figure 11. Concordia diagram for sample 07CYA-M133a. Magmatic zircons are shown as unfilled ellipses; inherited zircons are shown in light grey. See text for discussion.

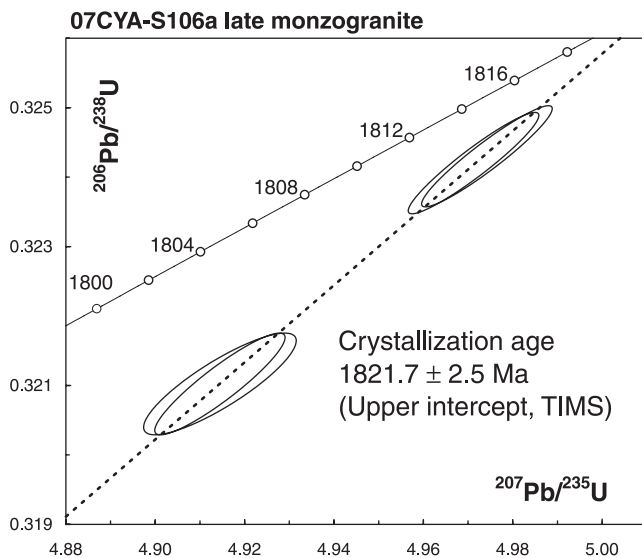


Figure 12. Concordia diagram for sample 07CYA-S106a.

time of crystallization and a minimum age of penetrative deformation. This agrees with *in situ* monazite results that suggest pervasive D_2 deformation ended shortly after ca. 1.84 Ga (Berman et al., in press).

CONCLUSIONS

1. Archean rocks form a component of Southampton Island and are documented here as comprising both northern (07CYA-M62a) and eastern (07CYA-B47c) parts of the basement complex. The profound influence of a Meso- to Eoarchean substrate is documented by extensive zircon detritus and inheritance and widespread ancient Sm-Nd model ages (Whalen et al., in press).
2. Geochronological data presented here document at least two sedimentary packages: an Archean psammite-semipelite sequence older than 2682 ± 17 Ma, and a carbonate-quartzite (continental margin?) sequence younger than 2615 ± 17 Ma. We are currently unable to determine if this younger sequence was deposited in the Archean or Paleoproterozoic. An aphanitic epiclastic rock may be time-equivalent to the younger sequence, however their dissimilar provenance profiles indicate distinct source regions.
3. At least three mafic-ultramafic plutonic events are documented: 1) a pre-1930 Ma event cut by quartz porphyry, 2) a 1870 ± 10 Ma gabbro-anorthosite event, and 3) a 1842 ± 5 Ma diorite event.
4. At one locality, orthopyroxene-bearing granodiorite is dated at 1931 ± 19 Ma. This is coeval with the quartz porphyry from the southern inlier, suggesting these regions experienced a similar magmatic event at ca. 1930 Ma.
5. Regional penetrative D_2 strain across Southampton Island is bracketed between ca. 1.85–1.84 Ga (the ages of S_2 foliated granodiorite and quartz diorite, respectively) and 1821.7 ± 2.5 Ma, the age of an undeformed to very weakly deformed monzogranite.

ACKNOWLEDGMENTS

This project was funded by the GSC's Northern Mineral Resources and Development Program, the Canada-Nunavut Geoscience Office, and the Polar Continental Shelf Program. Don James, Rob Berman and Joe Whalen contributed to our understanding of the area through fruitful discussions both in the field and in the office. We thank Pat Hunt, Tom Pestaj and the staff of the Geochronology Laboratory for their expert assistance in acquiring SEM, SHRIMP, and TIMS results respectively. The manuscript was improved by careful reviews by Rob Berman and Nancy Joyce.

REFERENCES

- Berman, R.G., Sanborn-Barrie, M., Stern, R.A., and Carson, C.J., 2005. Tectonometamorphism at ca. 2.35 and 1.85 Ga in the Rae Domain, western Churchill Province, Nunavut, Canada; insights from structural, metamorphic and in situ geochronological analysis of the southwestern Committee Bay Belt; *Canadian Mineralogist*, v. 43, p. 409–442. doi:10.2113/gscanmin.43.1.409
- Berman, R.G., Rayner, N., Sanborn-Barrie, M., and Chakungal, J., in press. New constraints on the tectonothermal history of Southampton Island, Nunavut, provided by in situ SHRIMP geochronology and thermobarometry; *Geological Survey of Canada, Current Research 2011-6*.
- Bröcker, M. and Enders, M., 1999. U-Pb zircon geochronology of unusual eclogite-facies rocks from Syros and Tinos (Cyclades, Greece); *Geological Magazine*, v. 136, p. 111–118. doi:10.1017/S0016756899002320
- Chakungal, J., Sanborn-Barrie, M., and James, D., 2007. Southampton Island: An Updated Geosciences Database; 35th Annual Yellowknife Geoscience Forum Abstracts; Northwest Territories Geoscience Office, Yellowknife, NT, YKGSF Abstracts Volume 2007.
- Chakungal, J., Sanborn-Barrie, M., James, D., Rayner, N., Whalen, J., Craven, J., Spratt, J., Kosar, K., Ross, M., Zhang, S., and Coyle, M., 2008. Natural Resource Potential – Yes or No? Southampton Island Integrated Project: A Summary of 2007 & 2008 Results and Investigations; 36th Annual Yellowknife Geoscience Forum Abstracts; Northwest Territories Geoscience Office, Yellowknife, NT, YKGSF Abstracts Volume 2008.
- Corfu, F., Hanchar, J.M., Hoskin, P.W.O., and Kinny, P., 2003. Atlas of zircon textures; *Reviews in Mineralogy and Geochemistry*, v. 53, p. 469–500. doi:10.2113/0530469
- Davis, W.J., McNicoll, V.J., Bellerive, D.R., Santowski, K., and Scott, D.J., 1997. Modified chemical procedures for the extraction and purification of uranium from titanite, allanite, and rutile in the Geochronology Laboratory, Geological Survey of Canada; *in Current Research, Part F; Radiogenic age and isotopic studies: Report 10; Geological Survey of Canada, Paper 1997-F*, p. 33–35.
- Hoaglin, D.C., Mosteller, F., and Tukey, J.W., 1983. *Understanding Robust and Exploratory Data Analysis*; John Wiley & Sons, p. 345–349.
- Krogh, T.E., 1982. Improved accuracy of U-Pb zircon ages by the creation of more concordant systems using an air abrasion technique; *Geochimica et Cosmochimica Acta*, v. 46, p. 637–649. doi:10.1016/0016-7037(82)90165-X
- Ludwig, K.R., 2003. User's manual for Isoplot/Ex rev. 3.00: a geochronological toolkit for Microsoft Excel; Berkeley Geochronology Center, Special Publication 4, Berkeley, 70 p.
- Mezger, K., Hanson, G.N., and Bohlen, S.R., 1989. High-precision U-Pb ages of metamorphic rutile: application to the cooling history of high-grade terranes; *Earth and Planetary Science Letters*, v. 96, p. 106–118. doi:10.1016/0012-821X(89)90126-X
- Parrish, R.R., Roddick, J.C., Loveridge, W.D., and Sullivan, R.W., 1987. Uranium-lead analytical techniques at the geochronology laboratory, Geological Survey of Canada; *in Radiogenic Age and Isotopic Studies: Report 1; Geological Survey of Canada*, v. 87-2, p. 3–7.
- Rainbird, R.H., Davis, W.J., Pehrsson, S.J., Wodicka, N., Rayner, N., and Skulski, T., 2010. Early Paleoproterozoic supracrustal assemblages of the Rae domain, Nunavut, Canada: intracratonic basin development during supercontinent break-up and assembly; *Precambrian Research*, v. 181, p. 167–186. doi:10.1016/j.precamres.2010.06.005
- Roddick, J.C., 1987. Generalized numerical error analysis with applications to geochronology and thermodynamics; *Geochimica et Cosmochimica Acta*, v. 51, p. 2129–2135. doi:10.1016/0016-7037(87)90261-4
- Sanborn-Barrie, M., Chakungal, J., James, D., Whalen, J., Berman, R.G., and Craven, J., 2007. The geology of Southampton Island, Nunavut, with a NE Laurentia context; 35th Annual Yellowknife Geoscience Forum Abstracts; Northwest Territories Geoscience Office, Yellowknife, NT, YKGSF Abstracts Volume 2007.
- Sanborn-Barrie, M., Chakungal, J., James, D., Whalen, J., Rayner, N., Berman, R.G., Craven, J., and Coyle, M., 2008. New understanding of the geology and diamond prospectivity of Southampton Island, central Nunavut; 36th Annual Yellowknife Geoscience Forum Abstracts; Northwest Territories Geoscience Office, Yellowknife, NT, YKGSF Abstracts Volume 2008.
- Sanborn-Barrie, M., Chakungal, J., and Buller, G., 2009. Bedrock field data and photographic record of exposed Precambrian basement, Southampton Island, Nunavut; *Geological Survey of Canada, Open File 6177, 1 DVD*. doi:10.4095/247890
- Stacey, J.S. and Kramers, J.D., 1975. Approximation of terrestrial lead isotope evolution by a two stage model; *Earth and Planetary Science Letters*, v. 26, p. 207–221. doi:10.1016/0012-821X(75)90088-6
- Stern, R.A., 1997. The GSC Sensitive High Resolution Ion Microprobe (SHRIMP): analytical techniques of zircon U-Th-Pb age determinations and performance evaluation; *in Current Research, Part F; Radiogenic Age and Isotopic Studies, Report 10, Geological Survey of Canada, Paper 1997-F*, p. 1–31.
- Stern, R.A. and Amelin, Y., 2003. Assessment of errors in SIMS zircon U-Pb geochronology using a natural zircon standard and NIST SRM 610 glass; *Chemical Geology*, v. 197, p. 111–142. doi:10.1016/S0009-2541(02)00320-0
- Whalen, J.B., Sanborn-Barrie, M., and Chakungal, J., in press. Geochemical and Nd isotopic constraints from plutonic rocks on the magmatic and crustal evolution of Southampton Island, Nunavut; *Geological Survey of Canada, Current Research 2011-2*.
- Wyllie, P.J., 1981. Plate tectonics and magma genesis; *Geologische Rundschau*, v. 70, p. 128–153. doi:10.1007/BF01764318
- Yakymchuk, C., Sanborn-Barrie, M., Chakungal, J., and Jamieson, R.A., 2008. Petrology and tectonic significance of coronitic mafic granulites, Southampton Island, Nunavut; Atlantic Geoscience Society, 34th Colloquium and Annual Meeting, Dartmouth, NS, Program with Abstracts, 60.